

4-1-2008

Searching for zeroes: Unconventional superconductors in a magnetic field

I. Vekhter
Louisiana State University

A. Vorontsov
Louisiana State University

Follow this and additional works at: https://repository.lsu.edu/physics_astronomy_pubs

Recommended Citation

Vekhter, I., & Vorontsov, A. (2008). Searching for zeroes: Unconventional superconductors in a magnetic field. *Physica B: Condensed Matter*, 403 (5-9), 958-962. <https://doi.org/10.1016/j.physb.2007.10.237>

This Article is brought to you for free and open access by the Department of Physics & Astronomy at LSU Scholarly Repository. It has been accepted for inclusion in Faculty Publications by an authorized administrator of LSU Scholarly Repository. For more information, please contact ir@lsu.edu.

Searching for zeroes: unconventional superconductors in a magnetic field

I. Vekhter, A. Vorontsov

Department of Physics and Astronomy, Louisiana State University, Baton Rouge, LA 70803, USA

Abstract

We review the results of the microscopic approach to the calculation of the anisotropy in the specific heat in unconventional superconductors under rotated field. Treating vortex scattering on equal footing with the energy shift we find that the electronic specific heat may have minima or maxima when the field is aligned with the nodes, depending on the temperature and field range. We discuss the influence of the paramagnetic limiting and Fermi surface shape on the location of the inversion line.

Key words: Unconventional superconductivity; Vortex State; Specific heat; Thermal conductivity
PACS: 75.30.-m,75.30.Kz,75.50.Ee,77.80.-e,77.84.Bw

1. Introduction

One of the practical steps that help determine the origin of superconducting pairing in novel materials is the determination of the shape of the energy gap. There are few techniques that directly probe the location of the zeroes (nodes) of the superconducting gap in the bulk of unconventional superconductors. Prominent among them are measurements of the specific heat and the thermal conductivity under a rotated magnetic field. Here we review recent progress on theoretical underpinning of these experimental techniques, and their implication for realistic materials.

The basic idea underlying the measurements is based on the understanding that in superconductors with zeroes of the gap on the Fermi surface (FS) the unpaired quasiparticles have momenta close to those of the nodal directions. Specific heat (thermal conductivity) measure entropy (its transport), and are therefore insensitive to the condensate of Cooper pairs. Consequently, if an experiment selectively probes excitations over a region of the FS, it is able to help locate the gap nodes. Spectroscopic techniques (e. g. ARPES) can resolve the gap structure in quasi-2D systems with large gap; however, in materials with low T_c an alternative method is needed.

Magnetic field provides such an alternative. The field couples to the phase of the superconducting order parameter, and drives supercurrents that, in turn, affect near-nodal quasiparticles. In the mixed state, when the field is only weakly screened, the interplay between the supercurrents and single particle excitations occurs throughout the

bulk, and is therefore accessible experimentally.

In the semiclassical approach, valid at low fields, $H \ll H_{c2}$, and low temperatures, $T \ll T_c$, the position-dependent superflow around the vortices, $\mathbf{v}_s(\mathbf{r})$ shifts the energy of the unpaired electrons relative to the moving condensate, generating a finite field-dependent density of the quasiparticles. In the absence of the field the cost of a single electron excitation with momentum \mathbf{k} is $E_{\mathbf{k}} = \sqrt{\zeta_{\mathbf{k}}^2 + |\Delta_{\mathbf{k}}|^2}$, where $\zeta_{\mathbf{k}}$ is the band energy, and $\Delta_{\mathbf{k}}$ is the superconducting gap. In the presence of the Doppler shift due to slowly varying superflow this energy becomes $E'_{\mathbf{k}} = E_{\mathbf{k}} - \mathbf{v}_s(\mathbf{r}) \cdot \mathbf{k}$, and therefore some previously unoccupied states drop below the chemical potential and become populated. Since the Doppler shift outside of vortex cores is smaller than the maximal gap (supercurrent is below the pairbreaking value), the populated states are located near the gap nodes in the momentum space.

Pioneered by Volovik to predict that the density of states in a clean superconductors with lines of nodes varies as \sqrt{H} [1], this approach was extensively used to analyse nodal superconductors [2]. Early analysis aimed at high- T_c cuprates, and started with the assumption of a cylindrical Fermi surface with vertical line nodes. Vekhter et al. considered the field rotated with respect to nodes in the conducting planes, and showed that the density of states (DOS) varies with the angle of field rotation [3]. Since the superfluid velocity is always in the plane normal to the applied field, the Doppler shift for the nodal quasiparticles, $\mathbf{v}_s(\mathbf{r}) \cdot \mathbf{k}_n$, depends on the angle between the field and the nodal direction, and vanishes when the field is along the node. Consequently, the DOS was predicted to have a

minimum when the field is aligned with nodes, suggesting the measurements of the electronic specific heat as a test for the nodal directions. This behavior was indeed found in the vortex state of several unconventional superconductors [4]. The results were qualitatively consistent with the predictions of the semiclassical theory, even though the experiments were done at higher $T/T_c \geq 0.1$ and higher H/H_{c2} than the corresponding range in the cuprates.

Experiments on the anisotropy of thermal conductivity, $\kappa(H, T)$, under a rotated field continued for over 10 years, and unambiguously showed the superposition of the variation due to difference in transport normal and parallel to the vortices (“twofold”), and the additional features due to nodal structure [5]. Theoretical analysis of these measurements remained incomplete until recently. The Doppler shift approach leaves the lifetime in the absence of impurities infinite, and therefore does not account for the scattering on the vortices. The magnetic field does influence lifetime via the self-consistency between the DOS and the impurity scattering, so that the field dependence of κ is determined by the competition between the enhanced density of states and the change in lifetime. Consequently, it is not clear whether rotating the field through the nodes, for a fixed direction of the heat current, gives minima (as the DOS) or maxima (due to reduced scattering). Moreover, the connection between the local $\kappa(\mathbf{r})$ and the measured value $\kappa(\mathbf{H})$ for a given field direction is not fully established, and ‘ad hoc’ averaging procedures often entirely miss the twofold anisotropy.

The need for a complete theoretical analysis, accounting for the superflow beyond semiclassical treatment and addressing the scattering on the vortices, was emphasized by comparison of the data on the specific heat and the thermal conductivity anisotropy in heavy fermion CeCoIn₅, where the opposite gap structure was inferred from the specific heat [6] and thermal transport [7] measurements. Such a description was recently developed by us [8,9], and here we summarize the salient features of our approach, review the essential physics, and focus on a new aspect of the analysis, the effect of the Fermi surface shape.

2. Microscopic approach

Our approach is based on the quasiclassical formulation of the microscopic theory. In the spin and particle-hole space the matrix propagator, which depends on the direction at the Fermi surface (FS), $\hat{\mathbf{p}}$, and the center of mass coordinate, \mathbf{R} , and the mean field order parameter are

$$\hat{g}(\mathbf{R}, \hat{\mathbf{p}}; \varepsilon) = \begin{pmatrix} g & i\sigma_2 f \\ i\sigma_2 \underline{f} & -g \end{pmatrix}, \quad \hat{\Delta} = \begin{pmatrix} 0 & i\sigma_2 \Delta \\ i\sigma_2 \Delta^* & 0 \end{pmatrix}. \quad (1)$$

The equilibrium propagators obey

$$[(\varepsilon + \frac{e}{c} \mathbf{v}_F(\hat{\mathbf{p}}) \mathbf{A}(\mathbf{R})) \hat{\tau}_3 - \hat{\Delta}(\mathbf{R}, \hat{\mathbf{p}}) - \hat{\sigma}_{imp}(\mathbf{R}; \varepsilon), \hat{g}(\mathbf{R}, \hat{\mathbf{p}}; \varepsilon)] + i \mathbf{v}_F(\hat{\mathbf{p}}) \cdot \nabla_{\mathbf{R}} \hat{g}(\mathbf{R}, \hat{\mathbf{p}}; \varepsilon) = 0, \quad (2)$$

with the normalization condition $\hat{g}^2(\mathbf{R}, \hat{\mathbf{p}}; \varepsilon) = -\pi^2 \hat{1}$. In Eq.(2) $\mathbf{v}_F(\hat{\mathbf{p}})$ is the Fermi velocity for the direction $\hat{\mathbf{p}}$, the vector potential $\mathbf{A}(\mathbf{R})$ describes the applied field that we take to be uniform, and the impurity self-energy, $\hat{\sigma}_{imp}(\mathbf{R}; \varepsilon)$, is determined within the self-consistent t -matrix approximation. The order parameter is computed self-consistently with the separable pairing interaction $V(\hat{\mathbf{p}}, \hat{\mathbf{p}}') = V_0 \mathcal{Y}(\hat{\mathbf{p}}) \mathcal{Y}(\hat{\mathbf{p}}')$, where $\mathcal{Y}(\hat{\mathbf{p}})$ is the normalized basis function for the angular momentum representation. We consider quasi-two dimensional (open along z) Fermi surfaces and order parameters with vertical lines of nodes.

We model the vortex state by the extended Abrikosov solution consisting of superposition of both the lowest and higher Landau level functions, $\Phi_n(x)$, required for unconventional superconductors, $\Delta(\mathbf{R}) = \sum_n \Delta_n \langle \mathbf{R} | n \rangle$ with

$$\langle \mathbf{R} | n \rangle = \sum_{k_y} C_{k_y}^{(n)} \frac{e^{ik_y \sqrt{S_f} y}}{\sqrt[4]{S_f \Lambda^2}} \Phi_n \left(\frac{x - \Lambda^2 \sqrt{S_f} k_y}{\Lambda \sqrt{S_f}} \right). \quad (3)$$

For the field applied at an angle θ_H to the z -axis, the anisotropy factor $S_f = \sqrt{\cos^2 \theta_H + (v_{0\parallel}/v_{0\perp})^2 \sin^2 \theta_H}$, where $v_{0\perp}^2 = 2 \langle \mathcal{Y}^2(\hat{\mathbf{p}}) v_{\perp i}^2(p_z) \rangle_{FS}$, $v_{0\parallel}^2 = 2 \langle \mathcal{Y}^2(\hat{\mathbf{p}}) v_{\parallel}^2(p_z) \rangle_{FS}$, $\langle \bullet \rangle_{FS}$ denotes the Fermi surface average, v_{\parallel} is the projection of \mathbf{v}_F on the z axis, and $v_{\perp i}$ with $i = x, y$ is its projection on the axes normal to z .

We use the Brantd-Pesch-Tewordt (BPT) approximation in replacing the normal (diagonal) part of the propagator with its spatial average, solve for the off-diagonal components in terms of g , and use the normalization condition to determine the quasiclassical Green’s function. We then compute the density of states directly, and use the linear response theory in Keldysh formulation to determine the thermal conductivity. The justification of the approximation, and the technical details of the approach are given in Ref. [9] for a rotationally symmetric Fermi surface in the shape of a corrugated cylinder. Here we briefly review the main results of that work, discuss its relation to the data on CeCoIn₅, and focus on the influence of the Zeeman field and the shape of the Fermi surface on the conclusions and the phase diagram.

3. Results.

In Refs. [8,9] we considered a Fermi surface given by $p_f^2 = p_x^2 + p_y^2 - (r^2 p_f^2) \cos(2s p_z/r^2 p_f)$, with $s = r = 0.5$, and the d -wave gaps, $\mathcal{Y} = \sqrt{2} \cos 2\phi$, where ϕ is the azimuthal angle at the Fermi surface. The unexpected result of Ref.[8] was the inversion of the anisotropic profile of the specific heat across much of the phase diagram in the T - H plane. In the low temperature, low field region the results of the microscopic calculation agreed with that of the semiclassical approach, and the specific heat for the magnetic field applied along a nodal direction was lower than that for the field along a gap maximum. In contrast, upon increasing either the field or the temperature, the pattern changed and

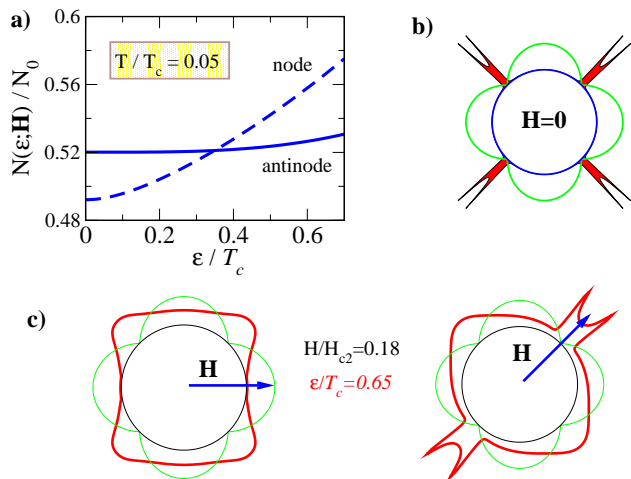


Fig. 1. Origin of the inversion of the specific heat anisotropy. a) Low-energy density of states for $H/H_{c2} = 0.18$ and field in the nodal and antinodal directions; b) Typical angle-resolved DOS (red) in zero field; c) Corresponding angle-resolved DOS (red) under applied field. The order parameter profile is shown for comparison (green).

the maximum, rather than a minimum of the specific heat was found when the field is aligned with the gap node. For a corrugated cylindrical Fermi surface reminiscent of that of CeCoIn_5 , the inversion occurred already at $T/T_c \sim 0.2$ at low fields, and $H/H_{c2} \sim 0.5$ at low temperature. Therefore over a very large part of the T - H phase diagram, away from the semiclassical low-energy regime, the theory predicts the anisotropy of the specific heat opposite to that expected at low fields. As a result we suggested that the measurements in CeCoIn_5 , performed at moderate H and T , were consistent with the $d_{x^2-y^2}$ symmetry. Our analysis of the thermal conductivity accounted for the first time both for the twofold anisotropy due to vortex scattering and for the structure due to nodes, and supported the $d_{x^2-y^2}$ symmetry of the order parameter.

The inversion is traced to the effect of vortex scattering as shown in Fig. 1. At low T the specific heat is related to the DOS $N(\hat{\mathbf{p}}, \varepsilon)/N_0 = -\text{Im}g(\hat{\mathbf{p}}, \varepsilon)$ via

$$C(T, \mathbf{H}) = \frac{1}{2} \int_{-\infty}^{+\infty} d\varepsilon \frac{\varepsilon^2 N(T, \mathbf{H}; \varepsilon)}{T^2 \cosh^2(\varepsilon/2T)} \quad (4)$$

and is most sensitive to the DOS at $\varepsilon \sim 2T$. Inversion of the $C(T, \mathbf{H})$ anisotropy at moderate T for a given H implies that the DOS anisotropy for the nodal and antinodal field directions changes sign, see Fig. 1a): at low (moderate) energies $N(\mathbf{H}||\text{node}, \varepsilon) < N(\mathbf{H}||\text{antinode}, \varepsilon)$ ($N(\mathbf{H}||\text{node}, \varepsilon) > N(\mathbf{H}||\text{antinode}, \varepsilon)$). Consider the angle-resolved density of states and recall that in the absence of the field the major contribution to $N(\varepsilon \ll T_c)$ is from the coherence peaks located at momenta $\hat{\mathbf{p}}_\varepsilon$ such that $\varepsilon = \Delta_0 \mathcal{V}(\hat{\mathbf{p}}_\varepsilon)$, close to the nodal directions, see Fig. 1b). Vortex scattering is weak for the quasiparticles traveling nearly parallel to the field, and strong for those with the momenta at moderate to large angles with respect to \mathbf{H} . Consequently, when the field is applied along a nodal

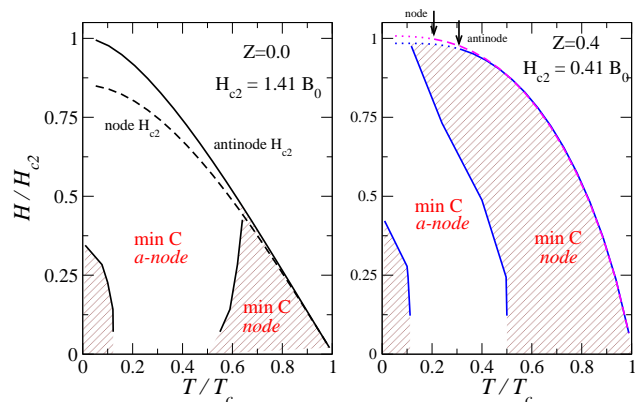


Fig. 2. Comparison of the phase diagram for the specific heat as a function of Zeeman splitting. In the shaded (unshaded) area $C(T, \mathbf{H})$ has a minimum for the field along the nodal (antinodal) direction. Here $B_0 = (ch/2e)/2\pi\xi_0^2$ with $\xi_0 = \hbar v_F/2\pi T_c$ is a measure of the orbital critical field. Parameter $Z = \mu B_0/2\pi T_c$ characterizes the strength of the Zeeman coupling. The arrows in the right panel indicate onset of the first order transition occurring for $Z \geq 0.35$.

direction, it largely preserves the spectral weight in the coherence peaks aligned with the field, while exciting unpaired quasiparticles at the other two nodes. In contrast, the field applied along the gap maxima induced more low energy states, but smears out the coherence peaks at moderate ε , transferring their spectral weight to other energies, see Fig. 1c). As a result, the DOS anisotropy changes sign at a finite ε^* , which was determined numerically.

While the results were very suggestive of the $d_{x^2-y^2}$ symmetry in CeCoIn_5 , specific details pertinent for this material left some questions open. First, the upper critical field in CeCoIn_5 is Pauli-limited [10], and spin splitting of the Fermi surface may be important. We considered its effect by including the Zeeman term, $v_z = g\mu_B \sigma \cdot \mathbf{H}$ with $g = 2$ into the semiclassical equations, and writing explicitly the equations for the two spin components, which are independent. On the other hand, the self-consistency involves spin summation. We found that the inclusion of Zeeman splitting modifies the location of the inversion lines in the phase diagram, but does not affect the main conclusion, namely, the inversion of the anisotropy at moderately low H and T , see Fig. 2. The effect of the paramagnetic limiting on the phase diagram is stronger at high fields and low temperatures due to “isotropization” of the upper critical field: the orbital limiting field differs for the nodal and antinodal orientation of the field, while the Pauli limiting field is direction-independent. Since in practice the measurements of the anisotropy are carried out at moderate fields, our conclusions remain substantially unmodified.

Second, the semiclassical analysis suggests that the local curvature of the Fermi surface around the nodal points affects the filling of the near-nodal states due to the field: for a fixed position and superflow $\mathbf{v}_s(\mathbf{r})$, the variation of the Fermi velocity $\mathbf{v}_F(\hat{\mathbf{p}})$ with direction $\hat{\mathbf{p}}$ near the node affects the Doppler shift. Moreover, in borocarbide superconductors some of the features of the anisotropy profile were suggested to be due to the nested parts of the Fermi

surface [11]. Consequently, we explored the influence of the Fermi surface geometry on our conclusions.

We consider a model two-dimensional Fermi surface given by $p_F^2 = p_x^2 + p_y^2 + a^2(p_x^4 + p_y^4)$, and chose $ap_F = 2$. In this case the directions along the axes and $p_x = p_y$ are inequivalent, and therefore the map of the specific heat anisotropy in the T - H plane depends on whether the order parameter is of the $d_{x^2-y^2}$ or d_{xy} type, with nodes along [110] or [100]. We consider both cases, and model the order parameter by $\Delta(p_x, p_y) = \Delta_0(p_x^2 - p_y^2)$ and $\Delta(p_x, p_y) = \Delta_0(2p_x p_y)$ respectively, with p_x, p_y at the FS. Therefore the nodes are located either in the “flat” (low curvature) or in the “corner” (high curvature) part of the Fermi surface.

While it is not possible to carry out the fully self-consistent calculation in field for a FS with no c -axis energy dispersion, we showed in Ref.[9] that solving for $\Delta_0(T, H = 0)$ and then modeling the vortex state by the lowest Landau Level with $\Delta(T, H) = \Delta_0(T, 0)\sqrt{1 - H/H_{c2}}$ gives results in semi-quantitative agreement with the self-consistent calculation for a corrugated FS. This is also seen from comparing the left panels of Fig. 2 (self-consistent, corrugated FS) and Fig. 3 (2D FS). We show the results in Fig. 3. It is clear from that the location of the anisotropy inversion lines is sensitive to the shape of the Fermi surface.

If the nodes of the gap are at the regions of high FS curvature, the “semiclassical” regime of minima of the specific heat for the field along the nodes is suppressed. Now even for the field along the node the near-nodal quasiparticles have the velocity at a substantial angle to the field direction, and are efficiently scattered by the vortices; hence the anisotropy crossover line is pushed to ultra-low fields, where we cannot detect it numerically. Over a large part of the phase diagram the minima of the specific heat correspond to the field along the gap maxima. Similarly to the rotationally symmetric Fermi surface, the anisotropy is reversed at low T and high fields, but in this region near the transition line the amplitude of the oscillations is small, and hence is of little experimental relevance.

In contrast, flattening of the near-nodal Fermi surface slightly extends the “semiclassical” region. In this geometry when the field is applied along a nodal direction, the Doppler shift nearly vanishes not just at the nodal point where \mathbf{k}_n is normal to the superfluid velocity, \mathbf{v}_s , but over the entire near-nodal region. Moreover, the scattering of the quasiparticles on vortices in this region is small, since their velocity is nearly parallel to the field. As a result, semiclassical results have a somewhat extended regime of validity.

In CeCoIn₅ the FS is not rotationally symmetric [12], and likely locations of the nodes pass through regions of high curvature. Therefore the inversion line is likely to be at lower T, H , than a cylindrical FS model predicts.

4. Summary

We reviewed here recent progress in microscopic calculations of the electronic specific heat of unconventional su-

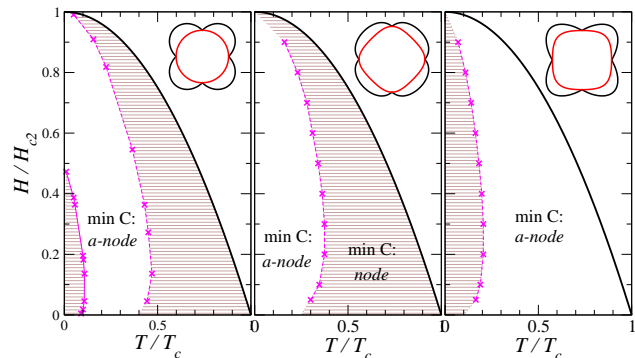


Fig. 3. Effect of the Fermi surface shape on the anisotropy map of the specific heat. Left panel: cylindrical Fermi surface; middle panel: nodes in the region of high curvature; right panel: nodes in the region of low curvature. In the shaded (unshaded) area $C(T, \mathbf{H})$ has a minimum for the field along the nodal (antinode) direction.

perconductors under a rotated magnetic field, and its connection with the experimental efforts to use the method for determination of the nodal directions. The approach uses the Brandt-Pesch-Tewordt approximation, which is nearly exact at high fields, and likely overestimated the effect of vortex scattering at low fields. The major difference with the results of the semiclassical approximation is the inversion of the anisotropy of the density of states and the specific heat due to the competition between the Doppler energy shift and spectral weight redistribution resulting from scattering on the vortices. The low-to-moderate T and H location of the inversion line makes it of experimental relevance, and we showed that the field and temperature range of this inversion is weakly dependent of paramagnetic effects, but is sensitive to the shape of the Fermi surface. A more complete analysis of the Fermi surface effects and Zeeman splitting, including the behavior of the thermal conductivity, will be published elsewhere.

We benefited from enlightening discussions with Y. Matsuda and T. Sakakibara. This research was supported in part by the Louisiana Board of Regents.

References

- [1] G. E. Volovik, JETP Letters **58** (1993) 469.
- [2] C. Kübert and P. J. Hirschfeld, Phys. Rev. Lett. **80** (1998) 4963; Sol. State. Commun. **105** (1998) 459.
- [3] I. Vekhter et al., Phys. Rev. B **59** (1999) R9023; *ibid.* **64** (2001) 064513.
- [4] T. Park et al., Phys. Rev. Lett. **90** (2003) 177001; T. Park and M. Salamon, Mod. Phys. Lett. B **18** (2004), 1205.
- [5] For a review, see Y. Matsuda et al., J. Phys. Cond. Mat. **18** (2006) R705.
- [6] H. Aoki et al., J. Phys. Cond. Mat. **16** (2004) L13.
- [7] K. Izawa et al. Phys. Rev. Lett. **87** (2001) 057002.
- [8] A. Vorontsov and I. Vekhter, Phys. Rev. Lett. **96** (2006) 237001.
- [9] A. Vorontsov and I. Vekhter, cond-mat/0702225 (unpublished); cond-mat/0702226 (unpublished).
- [10] A. Bianchi et al., Phys. Rev. Lett. **89** (2002) 137002.
- [11] M. Udagawa et al., Phys. Rev. B **71** (2005) 024511.
- [12] Y. Haga et al. Phys. Rev. B **63** (2001) 060503(R).